● **RESEARCH ARTICLE**

Effect of glycosides of *Cistanche* on the expression of mitochondrial precursor protein and keratin type II cytoskeletal 6A in a rat model of vascular dementia

Yan-mei Zhang[1], Wei Wu[2], Wei Ma[3], Fang Wang[4], Jun Yuan[1, *]

1 Department of Neurology, Inner Mongolia Autonomous Region People's Hospital, Hohhot, Inner Mongolia Autonomous Region, China
2 Department of Brain Center, The Second Affiliated Hospital of Wenzhou Medical University, Wenzhou, Zhejiang Province, China
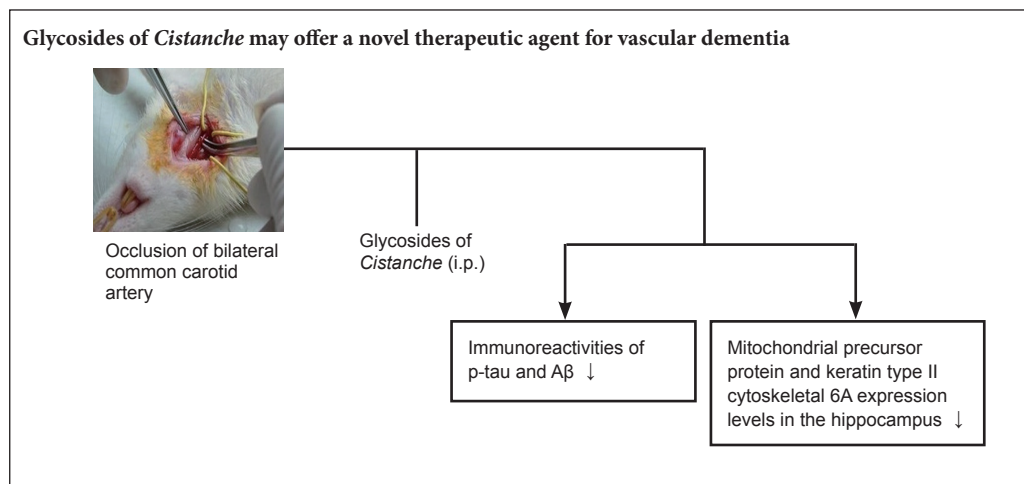3 First Hospital of Wuhan, Wuhan, Hubei Province, China
4 Jianghan University, Wuhan, Hubei Province, China

Graphical Abstract

Glycosides of *Cistanche* may offer a novel therapeutic agent for vascular dementia

Occlusion of bilateral common carotid artery

Glycosides of *Cistanche* (i.p.)

Immunoreactivities of p-tau and Aβ ↓

Mitochondrial precursor protein and keratin type II cytoskeletal 6A expression levels in the hippocampus ↓

Abstract

Glycosides of *Cistanche* (GC) is a preparation used extensively for its neuroprotective effect against neurological diseases, but its mechanisms of action remains incompletely understood. Here, we established a bilateral common carotid artery occlusion model of vascular dementia in rats and injected the model rats with a suspension of GC (10 mg/kg/day, intraperitoneally) for 14 consecutive days. Immunohistochemistry showed that GC significantly reduced p-tau and amyloid beta (Aβ) immunoreactivity in the hippocampus of the model rats. Proteomic analysis demonstrated upregulation of mitochondrial precursor protein and downregulation of keratin type II cytoskeletal 6A after GC treatment compared with model rats that had received saline. Western blot assay confirmed these findings. Our results suggest that the neuroprotective effect of GC in vascular dementia occurs *via* the promotion of neuronal cytoskeleton regeneration.

Key Words: nerve regeneration; vascular dementia; glycosides of Cistanche; mitochondrial precursor protein; keratin type II cytoskeletal 6A; proteomics; neuroprotection; neural regeneration

Introduction

Vascular dementia is the second most common type of dementia (Neltner et al., 2014; Sachdev et al., 2014; Tatlisumak et al., 2014; Sinclair et al., 2015; Thomas et al., 2015; Reijmer et al., 2016). The unremitting and irreversible memory damage that occurs in patients with vascular dementia leads to a severe deterioration in quality of life and places a heavy economic burden on the patient's family (Barker et al., 2014; Burke et al., 2014; Chen et al., 2014; Brandenburg et al., 2016). Prevention and treatment of the disease is increasing-

ly important in countries with aging populations. Therefore, there is increasing research interest in the search for effective drugs for the treatment of vascular dementia.

Cistanche is a plant used as a nootropic in traditional Chinese medical theory (Chen et al., 2014; Szalárdy et al., 2015; You et al., 2015). Glycosides of *Cistanche* (GC) is a preparation extracted from *Cistanche*. There is considerable evidence supporting the idea that GC can improve axonal regeneration (Procaccio et al., 2014; Love et al., 2015; Brandenburg et al., 2016; Gu et al., 2016). Numerous animal

studies have shown that GC enhances cognitive function (Procaccio et al., 2014; Talarowska et al., 2014; Fischer and Maier, 2015).

We previously used bilateral common carotid artery occlusion to establish rat models of vascular dementia. In this model, spatial learning and memory are significantly improved after intervention with GC (Chen et al., 2015). GC can also regulate and improve immunity, but is best known as a nerve tonic and memory enhancer (Chen et al., 2014; Procaccio et al., 2014; Szalárdy et al., 2015; You et al., 2015; Brandenburg et al., 2016).

However, few studies have investigated the molecular mechanisms underlying the effects of GC in vascular dementia. Here, we use proteomics to explore the relationship between proteins and vascular dementia, to determine the mechanism underlying the neuroprotective effect of GC.

Materials and Methods

Animals
Six-week-old adult male specific-pathogen-free Wistar rats ($n = 37$), weighing 230–270 g, were provided by the Experimental Animal Center, Hubei Province, China (license number: SYXK (E) 2014-0030). The experiment followed the National Guidelines for the Care and Use of Laboratory Animals, and the Consensus Author Guidelines on Animal Ethics and Welfare produced by the International Association of Veterinary Editors. The manuscript was prepared in accordance with the Animal Research: Reporting of In Vivo Experiments (ARRIVE) guidelines.

Rats were housed in groups of three per cage at 25°C with a 12-hour light/dark cycle and free access to food and water. Rats ($n = 37$) were randomly assigned to a control group ($n = 10$), a vascular dementia group ($n = 12$), and a vascular dementia + GC group (GC-treated, $n = 15$).

Establishment of rat models of vascular dementia
Under deep anesthesia with 10% chloral hydrate, bilateral common carotid arteries of rats in the vascular dementia and GC-treated groups were carefully separated from the surrounding tissues, then tightly ligated using 10-0 suture thread on both ends, and the common carotid arteries were cut. The rats in the control group were subjected to the same surgical procedure except that the common carotid arteries were exposed but not ligated. The Morris water maze was performed according to previously described methods to verify whether the animal model had been successfully established (Chen et al., 2015).

Pharmacological treatment
Cistanche powder (Certificate No. Z20050216, Sinphar Tian-Li Pharmaceutical Co., Ltd., Hangzhou, China) was mixed with ultrapure water and extracted by TF-2000C Ultrasonicator (Tuofen, Shanghai, China) (power 100%, 30°C, 40 minutes). GC concentration was measured by assaying phenylethanoid glycosides. After injury, all rats in the GC-treated group received GC (10 mg/kg/day, 1 mL, intraperitoneally, once daily) for 14 consecutive days. Rats

in the control and vascular dementia groups received saline (1 mL, intraperitoneally).

Immunohistochemistry
After 14 days of GC (or saline) administration, seven rats from each group were decapitated and the brains extracted. The cerebral cortices were removed and hippocampal tissue was carefully dissected out, and cut into 3-μm thick sections using freezing microtome. Sections of hippocampal tissue were fixed with 4% paraformaldehyde for 30–60 minutes, washed with PBS, and incubated in 3% H_2O_2 for 10 minutes followed by goat serum for 15 minutes, all at room temperature. Sections were then incubated in rabbit anti-rat phosphorylated p-tau primary antibody (1:1,000 in PBS; Bioworld Technology, Inc., TX, USA) and rabbit anti-rat amyloid beta (Aβ) primary antibody (1:1,000; Bioworld Technology, Inc.) in a wet box at 37°C for 2–3 hours, before incubation in the secondary antibody (goat anti-mouse IgG; Bioworld Technology, Inc.) for 15 minutes at room temperature. Specimens were visualized with 3,3′-diaminobenzidine tetrahydrochloride (Dako, Tokyo, Japan). Images were captured using a light microscope (Olympus, Tokyo, Japan) and processed using Photoshop (version 7.0; Adobe, San Jose, CA, USA). Immunopositive particles were brown, so brown staining in the cytoplasm was selected as positive reaction, and semi-quantification was carried out using an HMIAS-2000 image analysis system (Qianpin Co., Wuhan, China). In each specimen, five fields of view were selected at random and five positive cells were selected in each view and the average gray value was measured as a set of relative values.

Two-dimensional gel electrophoresis (2-DE)
After 14 days of GC or saline administration, eight rats from each group were anesthetized and decapitated, and the hippocampal tissues were quickly harvested and immediately frozen in liquid nitrogen. All tissues were homogenized in liquid nitrogen using a mortar and pestle, and collected in lysis buffer (7 M urea, 2 M thiourea, 2% CHAPS, 20 mM Tris). Insoluble particles were removed by centrifugation at 13,000 × g for 20 minutes at 4°C. Contaminated nucleic acid was disrupted by intermittent sonic oscillation for 5 minutes. Samples were centrifuged again under the same conditions and the supernatants were collected. Protein concentration was measured using the Bradford assay (Beyotime Inc., China) and the samples were store at −80°C until use.

To investigate the protein expression profile in the hippocampus, 2-DE was performed according to the manufacture's instructions (GE Healthcare, Pittsburgh, PA, USA). The protein solution (120 μg/sample) was adjusted with rehydration buffer for a final volume of 350 μL. Isoelectric focusing was performed using IPG strips (pH 4–7, size 22 cm) on an Ettan IPG phor II system (all from GE Ettan IPGphor3, GE Healthcare). Afterwards, the strips were equilibrated for 15 minutes.

2-DE was performed using 12.5% sodium dodecyl sul-

Table 1 Protein information of mitochondrial precursor protein and type II cytoskeletal 6A identified by time-of-flight mass spectrometry

Accession	Protein name	Function	T/C
gi|84781723	Mitochondrial precursor, heat shock protein 75 kDa	Chaperone that expresses an ATPase activity	2.54
gi|155369696	Keratin, type II cytoskeletal 6	Structural support to the epithelial cell	−1.58

phate (SDS) polyacrylamide gels (24 cm × 19.5 cm × 1.0 mm) with 0.5% agarose sealing glue in an Ettan DALTSix electrophoresis system (GE, Ettan DALTSix, GE Healthcare). Electrophoresis was carried out at 2 W for 45 minutes, followed by separation at 17 W for 4 hours until the bromophenol blue had nearly reached the bottom of 2-DE gel.

The gels were stained using silver nitrate (Damao Chemical Reagent Factory, Tianjin, China) and images were captured on a 2-DE image scanning system (VT, USA). Image Master 2D Platinum 5.0 software (GE, Inc., PA, USA) was used to scan and analyze the 2-DE image.

Protein spots were excised from the gel using an automated SpotPicker (GE, Inc.) after matching and identifying differences in protein points. Subsequently, peptide information was obtained using a 4700 MALDI TOF/TOF mass spectrometer (GE, Inc.).

Matrix-assisted laser desorption/ionization time-of-flight mass spectrometry

For peptide mass fingerprinting and subsequent analysis, gels were sliced and subjected to a slightly modified in-gel protocol as described in the manufacturer's instructions. There were methanol (Fisher M/4056/17), acetonitrile (Fisher A/0626/17), trypsin (Promega V5280), trypsin resolve solution (Promega V530), ammonium bicarbonate (Sigma A6141), C-18 ZipTip (Millipore ZTC18M096), and trifluoroacetic acid (GE HealthCare).

Briefly, protein spots were destained with destaining solution (30 mM $K_3Fe(CN)_6$:100 mM NaS_2O_3 = 1:1) and dehydrated with 100 mm ammonium bicarbonate and acetonitrile, reduced with trichloroethyl phosphate for 20 minutes at room temperature, and then alkylated in iodoacetic acid for 30 minutes in the dark. The gel was incubated in 50 μL of 12 ng/μL modified trypsin solution in 25 mM ammonium bicarbonate, pH 8.6, at 37°C overnight. Peptides were extracted from the gel plug with 1% formic acid/2% acetonitrile and concentrated using C-18 Zip-Tips. Afterwards, samples were prepared using a Prespotted AnchorChip (PAC96) target with an alpha-cyano-4-hydroxycinnamic acid matrix for 96 sample spots and 24 calibration spots. Mass spectrum peptide information was obtained using a 4700 MALDI TOF/TOF mass spectrometer. Resulting data were analyzed using a GPS Explorer (Applied Biosystems Inc., NY, USA), which invoked a MASCOT database search (Matrix Science, London, UK) using a mouse subset of the National Center for Biotechnology Information database.

Western blot assay

The hippocampus was prepared and protein concentration was measured as described above. Protein samples were loaded onto an SDS polyacrylamide gel, electrophoresed and transferred to a polyvinylidene difluoride membrane. The membrane was washed in Tris-buffered saline and Tween 20, blocked in 10% non-fat milk and 0.05% Tween in phosphate-buffered saline. The membranes were incubated overnight at 4°C with rabbit anti-mitochondrial precursor protein polyclonal antibody (1:2,000; Proteintech Inc., Chicago, IL, USA) and rabbit anti-keratin type II cytoskeletal 6A (KRT6A) polyclonal antibody (1:1,000; Proteintech Inc.) in 10% non-fat milk. The secondary antibody, horseradish peroxidase-conjugated goat anti-rabbit (Google Biotechnology Inc., Wuhan, Hubei Province, China) was diluted (1:2,000) in 10% non-fat milk and incubated at 25°C for 1 hour. Mouse anti-rat β-actin monoclonal antibody (1:2,000; Google Biotechnology Inc.) was used as an internal reference. A western blot scanning system (V300; EPSON, Nagano-ken, Japan), and AlphaEaseFC Adobe PhotoShop (Alpha Innotech, CA, USA) were used to determine mitochondrial precursor protein and KRT6A expression levels expressed as integrated optical density normalized to β-actin.

Statistical analysis

Quantitative data were expressed as the mean ± SD. Image-Master 2D Platinum 5.0 software (GE, Inc.) was used to scan and analyze the 2-DE information. Two-way analysis of variance was performed using GraphPad Prism 6.0 (GraphPad Software, Inc., La Jolla, CA, USA). $P < 0.05$ was considered statistically significant.

Results

Effects of GC on p-tau and Aβ immunoreactivity in the hippocampus of rat models of vascular dementia

Immunohistochemistry showed that p-tau and Aβ expression was greater after 14 days of treatment with GC than in the control group. However, expression of these proteins in the GC-treated group was significantly lower than that in the vascular dementia group ($P < 0.05$; **Figure 1**).

GC regulated expression of mitochondrial precursor protein and KRT6A in the hippocampus of rat models of vascular dementia

Expression of two proteins was significantly different in the GC-treated group than in the vascular dementia group: mitochondrial precursor protein (also known as heat shock protein (HSP) 75 kDa) was upregulated, and KRT6A was downregulated (**Figures 2**, **3**). Protein information is listed in **Table 1**.

Validation of proteomic data by western blot assay

Western blot results confirmed the data obtained by proteomics: mitochondrial precursor protein expression was greater, and KRT6A expression was lower, in the GC-treated group than in the vascular dementia group (**Figure 4**).

Discussion

Vascular dementia is a syndrome characterized by impairments in memory, behavior and cognition, and is mainly caused by cerebrovascular diseases (Barker et al., 2014; Burke et al., 2014; Oliveira et al., 2014; Szalárdy et al., 2015). The pathology common to all types of dementia, and responsible for its progression, is neurodegeneration (Foster et al., 2014; Fischer and Maier, 2015; Kalaria et al., 2015; Chen et al., 2016; Pérez-Hernández et al., 2016). Many plant extracts have therapeutic properties. The bioactivity of these compounds against neurodegeneration is mainly due to their antioxidant and anti-amyloidogenic effects (Fischer and Maier, 2015; You et al., 2015; Pérez-Hernández et al., 2016).

Cistanche is a Chinese herb that is used as a nootropic in traditional Chinese medicine. Emerging research indicates that *Cistanche* is beneficial in amnesia, specifically in the inhibition of memory loss progression (Procaccio et al., 2014; You et al., 2015; Pérez-Hernández et al., 2016). There is considerable evidence that GC can promote axonal regeneration and act as a nerve growth modulator (Talarowska et al., 2014; Gu et al., 2016; Xu et al., 2016). In our previous work using the Morris water maze, we found that the escape latency of rat models of vascular dementia decreased after treatment with GC, indicating that GC improves spatial learning ability. Although GC has been used extensively for its neuroprotective effect (Chen et al., 2015), the mechanism underlying this effect remains unclear.

It is well known that Aβ peptides and p-tau are highly expressed in senile plaques and neurofibrillary tangles. Aβ and tau proteins play key roles in the morphogenesis of neurons, but in certain pathological situations, they generate aberrant aggregates that are neurotoxic (Love et al., 2015; Sadigh-Eteghad et al., 2015; Sinclair et al., 2015; Thomas et al., 2015; Wang et al., 2015; Reijmer et al., 2016). The present immunohistochemistry results indicate that p-tau and Aβ protein expression in GC-treated rat models of vascular dementia was significantly greater than that in control rats, but lower than that in untreated model rats. Therefore, the neuroprotective effect of GC may occur by reducing the toxicity of Aβ and p-tau.

Our proteomic study in rat hippocampus revealed large differences in the expression of mitochondrial precursor protein, keratin, and KRT6A. In terms of function, we speculate that the neuroprotective effect of GC may be associated with the remodeling of dendritic spine structure.

Mitochondrial precursor protein belongs to the HSP70 family (Rao et al., 2014; Gutiérrez-Aguilar and Baines, 2015; McGeer and McGeer, 2015). HSP75 is involved in molecular chaperone activation and maturation, and maintains the stability and normal function of cells (Booth et al., 2014, 2016; Tavallai et al., 2015). Mitochondrial precursor protein

is thought to play an important role in the transduction of some signaling pathways (Reid et al., 2014; Booth et al., 2015a, b). Recent studies have revealed that the HSP90 family regulates the operating environment of mitochondrial protein folding (An et al., 2014; Liu and Landgraf, 2015; Roberts et al., 2015; Stary and Giffard, 2015). HSP75 is localized in mitochondria and inhibits the generation of oxygen free radicals (Radu et al., 2014; Holloway et al., 2016). Our results show that the expression of HSP75 in the GC-treated group was increased 2.54-fold, suggesting that GC plays an antioxidant role, improves cellular oxidative balance, and delays apoptosis. This finding provides interesting clues about the interactions of the mitochondrial chaperone protein with other proteins.

Another differently expressed protein was KRT6A. The keratins, also called cytokeratins, are intermediate filament proteins that create an insoluble dense meshwork through the cytoplasm, giving structural support to the epithelial cell (Haricharan et al., 2014; Rorke et al., 2015; Szymanski et al., 2015). However, cytokeratins also play an active role in various cellular survival processes (proliferation and apoptosis) (Zhu et al., 2013; Schwingshackl et al., 2015; Popov and Komianos, 2016). These proteins may undergo phosphorylation and are also part of the bridging contact between the epithelial cell and its microenvironment (Lessard et al., 2013; Gil Lorenzo et al., 2014; Zhou et al., 2014; Chakrabarti et al., 2015). CK6a is the dominant isoform in the mammary gland (Bramanti et al., 2015a, b, 2016) and is upregulated in healing wound edges of the skin, indicating that cytokeratin is involved in cellular proliferation and migration. However, we are the first to show downregulation of KRT6A in the hippocampus; KRT6A expression was decreased 1.58-fold in the GC-treated group compared with the vascular dementia group. Therefore, the neuroprotective effect of GC may be associated with inhibition of neuroglial hyperplasia during cerebrovascular ischemia.

Together, the results of our study suggest that GC exerts its learning and memory-promoting effects in rat models of vascular dementia by reducing the expression of Aβ and p-tau, thus weakening the accumulation of these two toxic proteins and, in turn, reducing neuronal toxicity. Furthermore, GC might regulate the expression of mitochondrial precursor protein and KRT6A, which are associated with synaptic cytoskeleton morphogenesis and mitochondrial energy metabolism. Therefore, our data provide new insight into the underlying mechanisms of GCs, highlighting the possibility of GCs having multiple targets, which offers a promising novel therapeutic option for the treatment of vascular dementia.
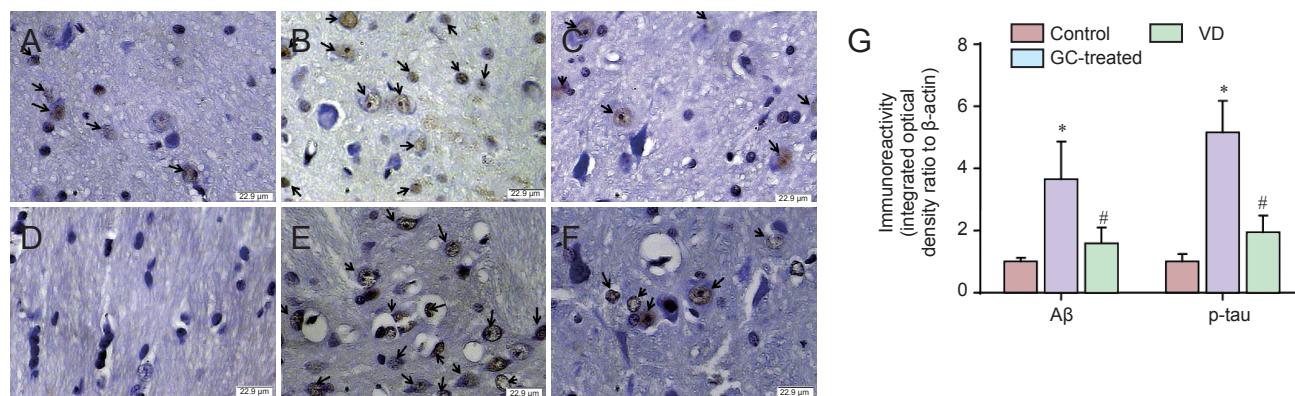
Figure 1 Effect of GCs on p-tau and Aβ immunoreactivity in the hippocampus of a rat model of vascular dementia.
(A–F) Representative immunohistochemical images for p-tau and Aβ staining. Cells immunopositive for p-tau (A–C) and Aβ (D–F) in control (A, D), vascular dementia model (B, E), and GC-treated (C, F) rats. Black arrows indicate immunopositive cells, with orange-brown staining in the cytoplasm indicating p-tau and Aβ imunoreactivity. (G) Average gray values of p-tau and Aβ in control rats, vascular dementia rats and CG-treated rats. p-tau and Aβ immunoreactivity was greater in the vascular dementia group than in the control group. This upregulation was significantly decreased after treatment with GC. Data are expressed as the mean ± SD. *P < 0.05, #P < 0.05 (two-way analysis of variance). Experiments were conducted in triplicate. GC: Glycosides of *Cistanche*; p-tau: phosphorylated tau; Aβ: amyloid beta; VD: vascular dementia.
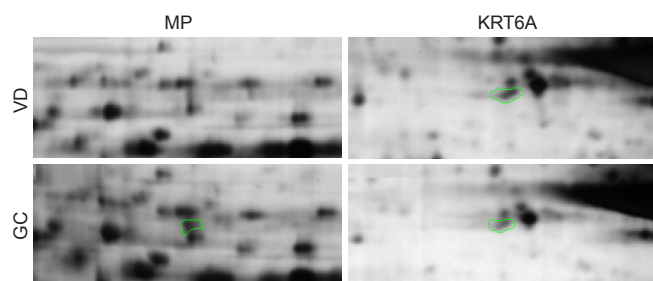

Figure 2 Two-dimensional gel electrophoresis profiles of mitochondrial precursor protein and KRT6A expression in rat models of vascular dementia with or without GC treatment
Panels show enlarged regions of the 2DE protein profile. Areas outlined in green show differently expressed protein points. Mitochondrial precursor protein expression was 2.54-fold greater in the GC-treated group than in the model group. KRT6A expression was 1.58-fold lower than in the model group. Proteomic studies were conducted in triplicate. MP: Mitochondrial precursor protein; KRT6A: keratin type II cytoskeletal 6A.

References

An J, Haile WB, Wu F, Torre E, Yepes M (2014) Tissue-type plasminogen activator mediates neuroglial coupling in the central nervous system. Neuroscience 257:41-48.

Barker R, Ashby EL, Wellington D, Barrow VM, Palmer JC, Kehoe PG, Esiri MM, Love S (2014) Pathophysiology of white matter perfusion in Alzheimer's disease and vascular dementia. Brain 137:1524-1532.

Booth L, Roberts JL, Cruickshanks N, Grant S, Poklepovic A, Dent P (2014) Regulation of OSU-03012 toxicity by ER stress proteins and ER stress-inducing drugs. Mol Cancer Ther 13:2384-2398.

Booth L, Roberts JL, Tavallai M, Nourbakhsh A, Chuckalovcak J, Carter J, Poklepovic A, Dent P (2015a) OSU-03012 and Viagra treatment inhibits the activity of multiple chaperone proteins and disrupts the blood-brain barrier: implications for anti-cancer therapies. J Cell Physiol 230:1982-1998.

Booth L, Roberts JL, Cash DR, Tavallai S, Jean S, Fidanza A, Cruz-Luna T, Siembiba P, Cycon KA, Cornelissen CN, Dent P (2015b) GRP78/BiP/HSPA5/Dna K is a universal therapeutic target for human disease. J Cell Physiol 230:1661-1676.

Booth L, Shuch B, Albers T, Roberts JL, Tavallai M, Proniuk S, Zukiwski A, Wang D, Chen CS, Bottaro D, Ecroyd H, Lebedyeva IO, Dent P (2016) Multi-kinase inhibitors can associate with heat shock proteins through their NH2-termini by which they suppress chaperone function. Oncotarget 7:12975-12996.

Bramanti V, Grasso S, Tibullo D, Giallongo C, Raciti G, Viola M, Avola R (2015a) Modulation of extracellular signal-related kinase, cyclin D1, glial fibrillary acidic protein, and vimentin expression in estradiol-pretreated astrocyte cultures treated with competence and progression growth factors. J Neurosci Res 93:1378-1387.

Bramanti V, Grasso S, Tomassoni D, Traini E, Raciti G, Viola M, Li Volti G, Campisi A, Amenta F, Avola R (2015b) Effect of growth factors and steroid hormones on heme oxygenase and cyclin D1 expression in primary astroglial cell cultures. J Neurosci Res 93:521-529.

Bramanti V, Grasso S, Tibullo D, Giallongo C, Pappa R, Brundo MV, Tomassoni D, Viola M, Amenta F, Avola R (2016) Neuroactive molecules and growth factors modulate cytoskeletal protein expression during astroglial cell proliferation and differentiation in culture. J Neurosci Res 94:90-98.

Brandenburg S, Muller A, Turkowski K, Radev YT, Rot S, Schmidt C, Bungert AD, Acker G, Schorr A, Hippe A, Miller K, Heppner FL, Homey B, Vajkoczy P (2016) Resident microglia rather than peripheral macrophages promote vascularization in brain tumors and are source of alternative pro-angiogenic factors. Acta Neuropathol 131:365-378.

Burke MJ, Nelson L, Slade JY, Oakley AE, Khundakar AA, Kalaria RN (2014) Morphometry of the hippocampal microvasculature in post-stroke and age-related dementias. Neuropathol Appl Neurobiol 40:284-295.

Chakrabarti KR, Whipple RA, Boggs AE, Hessler LK, Bhandary L, Vitolo MI, Thompson K, Martin SS (2015) Pharmacologic regulation of AMPK in breast cancer affects cytoskeletal properties involved with microtentacle formation and re-attachment. Oncotarget 6:36292-36307.
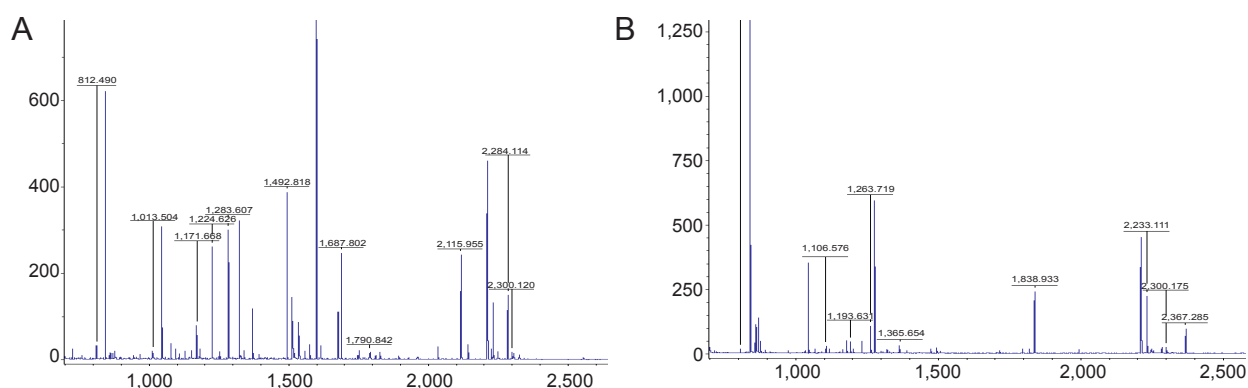
Figure 3 Peptide mass fingerprinting.
After destained and dehydrated, peptides were extracted and concentrated using C-18 Zip-Tips. Samples were prepared using a prespotted Anchor-Chip (PAC96) target. Mass spectrum peptide information was obtained using a 4700 MALDI TOF/TOF mass spectrometer. Peptide mass fingerprinting of (A) mitochondrial precursor protein; (B) KRT6A (type II cytoskeletal 6A) were listed above.
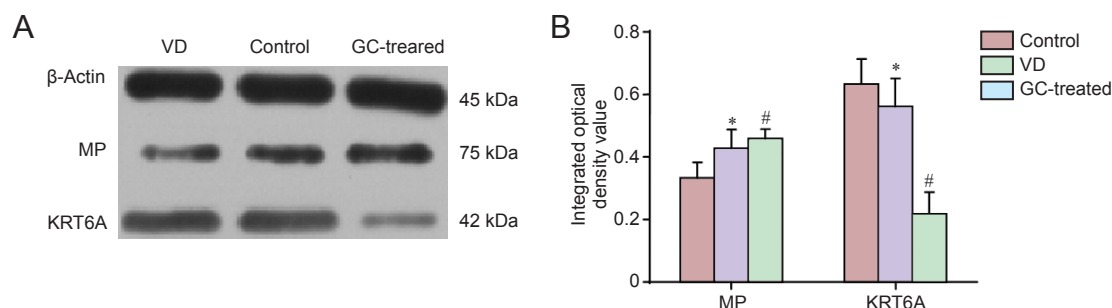

Figure 4 Western blot assay of mitochondrial precursor protein and KRT6A in the hippocampus of rat models of vascular dementia.
Data are expressed as the mean ± SD. *$P < 0.05$, *vs.* control group; #$P < 0.05$, *vs.* VD group (two-way analysis of variance). Western blot assays were conducted in triplicate. GC: Glycosides of *Cistanche*; VD: vascular dementia; MP: mitochondrial precursor protein; KRT6A: keratin type II cytoskeletal 6A.

Chen A, Akinyemi RO, Hase Y, Firbank MJ, Ndung'u MN, Foster V, Craggs LJ, Washida K, Okamoto Y, Thomas AJ, Polvikoski TM, Allan LM, Oakley AE, O'Brien JT, Horsburgh K, Ihara M, Kalaria RN (2016) Frontal white matter hyperintensities, clasmatodendrosis and gliovascular abnormalities in ageing and post-stroke dementia. Brain 139:242-258.

Chen J, Zhou SN, Zhang YM, Feng YL, Wang S (2015) Glycosides of cistanche improve learning and memory in the rat model of vascular dementia. Eur Rev Med Pharmacol Sci 19:1234-1240.

Chen S, Yin ZJ, Jiang C, Ma ZQ, Fu Q, Qu R, Ma SP (2014) Asiaticoside attenuates memory impairment induced by transient cerebral ischemia-reperfusion in mice through anti-inflammatory mechanism. Pharmacol Biochem Behav 122:7-15.

Fischer R, Maier O (2015) Interrelation of oxidative stress and inflammation in neurodegenerative disease: role of TNF. Oxid Med Cell Longev 2015:610813.

Foster V, Oakley AE, Slade JY, Hall R, Polvikoski TM, Burke M, Thomas AJ, Khundakar A, Allan LM, Kalaria RN (2014) Pyramidal neurons of the prefrontal cortex in post-stroke, vascular and other ageing-related dementias. Brain 137:2509-2521.

Gil Lorenzo AF, Bocanegra V, Benardon ME, Cacciamani V, Valles PG (2014) Hsp70 regulation on Nox4/p22phox and cytoskeletal integrity as an effect of losartan in vascular smooth muscle cells. Cell Stress Chaperones 19:115-134.

Gu C, Yang X, Huang L (2016) Cistanches herba: a neuropharmacology review. Front Pharmacol 7:289.

Gutiérrez-Aguilar M, Baines CP (2015) Structural mechanisms of cyclophilin D-dependent control of the mitochondrial permeability transition pore. Biochim Biophys Acta 1850:2041-2047.

Haricharan S, Hein SM, Dong J, Toneff MJ, Aina OH, Rao PH, Cardiff RD, Li Y (2014) Contribution of an alveolar cell of origin to the high-grade malignant phenotype of pregnancy-associated breast cancer. Oncogene 33:5729-5739.

Holloway KR, Sinha VC, Bu W, Toneff M, Dong J, Peng Y, Li Y (2016) Targeting oncogenes into a defined subset of mammary cells demonstrates that the initiating oncogenic mutation defines the resulting tumor phenotype. Int J Biol Sci 12:381-388.

Kalaria RN, Ferrer I, Love S (2015) Vascular disease, hypoxia and related conditions. In: Greenfield's Neuropathology (Love S, Perry A, Ironside J, Budka H, eds). London: CRC.

Lessard JC, Pina-Paz S, Rotty JD, Hickerson RP, Kaspar RL, Balmain A, Coulombe PA (2013) Keratin 16 regulates innate immunity in response to epidermal barrier breach. Proc Natl Acad Sci U S A 110:19537-19542.

Liu W, Landgraf R (2015) Phosphorylated and unphosphorylated serine 13 of CDC37 stabilize distinct interactions between its client and HSP90 binding domains. Biochemistry 54:1493-1504.

Love S, Chalmers K, Ince P, Esiri M, Attems J, Kalaria R, Jellinger K, Yamada M, McCarron M, Minett T, Matthews F, Greenberg S, Mann D, Kehoe PG (2015) Erratum: Development, appraisal, validation and implementation of a consensus protocol for the assessment of cerebral amyloid angiopathy in post-mortem brain tissue. Am J Neurodegener Dis 4:49.

McGeer PL, McGeer EG (2015) Targeting microglia for the treatment of Alzheimer's disease. Expert Opin Ther Targets 19:497-506.

Neltner JH, Abner EL, Baker S, Schmitt FA, Kryscio RJ, Jicha GA, Smith CD, Hammack E, Kukull WA, Brenowitz WD, Van Eldik LJ, Nelson PT (2014) Arteriolosclerosis that affects multiple brain regions is linked to hippocampal sclerosis of ageing. Brain 137:255-267.

Oliveira NR, Marques SO, Luciano TF, Pauli JR, Moura LP, Caperuto E, Pieri BL, Engelmann J, Scaini G, Streck EL, Lira FS, Pinho RA, Ropelle ER, Silva AS, De Souza CT (2014) Treadmill training increases SIRT-1 and PGC-1 alpha protein levels and AMPK phosphorylation in quadriceps of middle-aged rats in an intensity-dependent manner. Mediators Inflamm 2014:987017.

Pérez-Hernández J, Zaldívar-Machorro VJ, Villanueva-Porras D, Vega-Ávila E, Chavarría A (2016) A potential alternative against neurodegenerative diseases: phytodrugs. Oxid Med Cell Longev 2016:8378613.

Popov K, Komianos J (2016) MEDYAN: mechanochemical simulations of contraction and polarity alignment in actomyosin networks. PLoS Comput Biol 12:e1004877.

Procaccio V, Bris C, Chao de la Barca JM, Oca F, Chevrollier A, Amati-Bonneau P, Bonneau D, Reynier P (2014) Perspectives of drug-based neuroprotection targeting mitochondria. Rev Neurol (Paris) 170:390-400.

Radu M, Semenova G, Kosoff R, Chernoff J (2014) PAK signalling during the development and progression of cancer. Nat Rev Cancer 14:13-25.

Rao VK, Carlson EA, Yan SS (2014) Mitochondrial permeability transition pore is a potential drug target for neurodegeneration. Biochim Biophys Acta 1842:1267-1272.

Reid SP, Shurtleff AC, Costantino JA, Tritsch SR, Retterer C, Spurgers KB, Bavari S (2014) HSPA5 is an essential host factor for Ebola virus infection. Antiviral Res 109:171-174.

Reijmer YD, van Veluw SJ, Greenberg SM (2016) Ischemic brain injury in cerebral amyloid angiopathy. J Cereb Blood Flow Metab 36:40-54.

Roberts JL, Tavallai M, Nourbakhsh A, Fidanza A, Cruz-Luna T, Smith E, Siembida P, Plamondon P, Cycon KA, Doern CD, Booth L, Dent P (2015) GRP78/Dna K is a target for nexavar/stivarga/votrient in the treatment of human malignancies, viral infections and bacterial diseases. J Cell Physiol 230:2552-2578.

Rorke EA, Adhikary G, Young CA, Rice RH, Elias PM, Crumrine D, Meyer J, Blumenberg M, Eckert RL (2015) Structural and biochemical changes underlying a keratoderma-like phenotype in mice lacking suprabasal AP1 transcription factor function. Cell Death Dis 6:e1647.

Sachdev P, Kalaria R, O'Brien J, Skoog I, Alladi S, Black SE, Blacker D, Blazer DG, Chen C, Chui H, Ganguli M, Jellinger K, Jeste DV, Pasquier F, Paulsen J, Prins N, Rockwood K, Roman G, Scheltens P, Internationlal Society for Vascular Behavioral and Cognitive Disorders (2014) Diagnostic criteria for vascular cognitive disorders: a VASCOG statement. Alzheimer Dis Assoc Disord 28:206-218.

Sadigh-Eteghad S, Sabermarouf B, Majdi A, Talebi M, Farhoudi M, Mahmoudi J (2015) Amyloid-beta: a crucial factor in Alzheimer's disease. Med Princ Pract 24:1-10.

Schwingshackl A, Roan E, Teng B, Waters CM (2015) TREK-1 regulates cytokine secretion from cultured human alveolar epithelial cells independently of cytoskeletal rearrangements. PLoS One 10:e0126781.

Sinclair LI, Tayler HM, Love S (2015) Synaptic protein levels altered in vascular dementia. Neuropathol Appl Neurobiol 41:533-543.

Stary CM, Giffard RG (2015) Advances in astrocyte-targeted approaches for stroke therapy: an emerging role for mitochondria and microRNAS. Neurochem Res 40:301-307.

Szalárdy L, Zádori D, Klivényi P, Toldi J, Vécsei L (2015) Electron transport disturbances and neurodegeneration: from Albert Szent-Gyorgyi's Concept (Szeged) till novel approaches to boost mitochondrial bioenergetics. Oxid Med Cell Longev 2015:498401.

Szymanski WG, Zauber H, Erban A, Gorka M, Wu XN, Schulze WX (2015) Cytoskeletal components define protein location to membrane microdomains. Mol Cell Proteomics 14:2493-2509.

Talarowska M, Bobinska K, Zajaczkowska M, Su KP, Maes M, Galecki P (2014) Impact of oxidative/nitrosative stress and inflammation on cognitive functions in patients with recurrent depressive disorders. Med Sci Monit 20:110-115.

Tatlisumak T, Putaala J, Debette S (2014) Less common causes of stroke: diagnosis and management. In: Oxford Textbook of Stroke and Cerebrovasular Disease (Norrving B, ed), pp 153-162. Oxford: Oxford University Press.

Tavallai M, Hamed HA, Roberts JL, Cruickshanks N, Chuckalovcak J, Poklepovic A, Booth L, Dent P (2015) Nexavar/Stivarga and viagra interact to kill tumor cells. J Cell Physiol 230:2281-2298.

Thomas T, Miners S, Love S (2015) Post-mortem assessment of hypoperfusion of cerebral cortex in Alzheimer's disease and vascular dementia. Brain 138:1059-1069.

Wang Y, Lin J, Chen QZ, Zhu N, Jiang DQ, Li MX, Wang Y (2015) Overexpression of mitochondrial Hsp75 protects neural stem cells against microglia-derived soluble factor-induced neurotoxicity by regulating mitochondrial permeability transition pore opening in vitro. Int J Mol Med 36:1487-1496.

Xu Q, Fan W, Ye SF, Cong YB, Qin W, Chen SY, Cai J (2016) Cistanche tubulosa Protects Dopaminergic Neurons through Regulation of Apoptosis and Glial Cell-Derived Neurotrophic Factor: in vivo and in vitro. Front Aging Neurosci 8:295.

You SP, Zhao J, Ma L, Tudimat M, Zhang SL, Liu T (2015) Preventive effects of phenylethanol glycosides from Cistanche tubulosa on bovine serum albumin-induced hepatic fibrosis in rats. Daru 23:52.

Zhou Q, Anderson C, Zhang H, Li X, Inglis F, Jayagopal A, Wang S (2014) Repression of choroidal neovascularization through actin cytoskeleton pathways by microRNA-24. Mol Ther 22:378-389.

Zhu M, Lu C, Li W (2013) Transient exposure to echinacoside is sufficient to activate Trk signaling and protect neuronal cells from rotenone. J Neurochem 124:571-580.

Copyedited by Slone-Murphy J, Frenchman B, Yu J, Li CH, Qiu Y, Song LP, Zhao M